

Chemical Science

Accepted Manuscript



This is an *Accepted Manuscript*, which has been through the Royal Society of Chemistry peer review process and has been accepted for publication.

Accepted Manuscripts are published online shortly after acceptance, before technical editing, formatting and proof reading. Using this free service, authors can make their results available to the community, in citable form, before we publish the edited article. We will replace this *Accepted Manuscript* with the edited and formatted *Advance Article* as soon as it is available.

You can find more information about *Accepted Manuscripts* in the [Information for Authors](#).

Please note that technical editing may introduce minor changes to the text and/or graphics, which may alter content. The journal's standard [Terms & Conditions](#) and the [Ethical guidelines](#) still apply. In no event shall the Royal Society of Chemistry be held responsible for any errors or omissions in this *Accepted Manuscript* or any consequences arising from the use of any information it contains.

EDGE ARTICLE

A comparative study of the coordination behavior of *cyclo*-P₅ and *cyclo*-As₅ ligand complexes towards the trinuclear Lewis acid complex (perfluoro-*ortho*-phenylene)mercury

Cite this: DOI: 10.1039/x0xx00000x

Received 00th January 2014,
Accepted 00th January 2014

DOI: 10.1039/x0xx00000x

www.rsc.org/

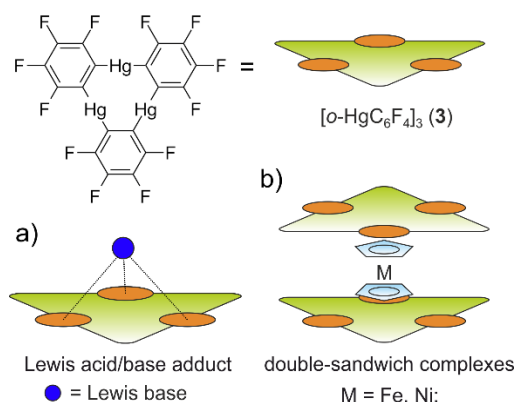
Martin Fleischmann,^a James S. Jones,^b François P. Gabbaï^b and Manfred Scheer^{a*}

Reactions of the *cyclo*-E₅ sandwich complexes [Cp^RFe(η⁵-P₅)] (**1**) and [Cp^RFe(η⁵-As₅)] (**2**) with the planar Lewis acid trimeric (perfluoro-*ortho*-phenylene)mercury [(*o*-C₆F₄Hg)₃] (**3**) afford compounds that show distinctly different assemblies in the solid state. The phosphorus ligand **1** forms dimeric coordination units with two molecules of **3**, with one P atom of each P₅ positioned in close proximity to the center of a molecule of **3**. In contrast to the coordination behavior of **1**, the arsenic analog **2** shows simultaneous interaction of three As atoms with the Hg atoms of **3**. A DFT study and subsequent AIM analyses of the products suggest that electrostatic forces are prevalent over donor-acceptor interactions in these adducts, and may play a role in the differences in the observed coordination behavior. Subsequently, a series of [Cp^RFe(η⁵-P₅)] (Cp^R = C₅H_{5-*n*}tBu_{*n*}, *n* = 1-3, **6 a-c**) sandwich complexes was prepared and also reacted with [(*o*-C₆F₄Hg)₃]. In the solid state the obtained products **7 a-c** with increasing steric demand of the Cp^R ligands show no significant change of the assembly compared to the Cp* analog **4**. All products were characterized by single crystal X-ray structure analysis, mass spectrometry, and elemental analysis as well as NMR spectroscopy and IR spectroscopy.

Introduction

The research area of substituent-free group 15 element ligands in the coordination sphere of transition metal complexes has shown to be a prosperous field in chemistry.¹⁻⁵ Some of these complexes possess planar E₃, E₄, E₅ and E₆ rings. From their appealing symmetry, to the lively discussion of their possible aromaticity,⁶⁻¹⁰ these main group ligands induce a fascination to chemists on their own. Among these, the ferrocene analogues sandwich complexes [Cp^RFe(η⁵-E₅)] (E = P (**1**), E = As (**2**))^{11,12} bearing a planar E₅ ring as an end-deck are even of special interest as ligands in supramolecular coordination chemistry, since they show a large variety of coordination modes of the *cyclo*-E₅ moieties depending on the nature of the used Lewis acid. While reactions of the *cyclo*-P₅ complex **1** with strongly coordinating Cu^I halides leads to an abundance of coordination polymers,^{13,14} and also spherical aggregates,¹⁵⁻¹⁹ the As analogue **2** leads only to the isolation of coordination polymers so far.²⁰ In these products the P atoms are mainly σ coordinating the Cu centers via their lone pairs while the As₅ ring mainly shows π coordination via As-As bonds. The reaction of **1** with Ag⁺ ions under weakly coordinating conditions affords a soluble one-dimensional coordination polymer.²¹ Recently, we were able to show that both E₅

complexes **1** and **2** reveal a similar η⁵-coordination of the E₅ end-deck to the group 13 cations Tl⁺ and In⁺.^{22,23} Since investigations of the reactivity of *cyclo*-P₅ and *cyclo*-As₅ complexes including a direct comparison are rare, it seems worthwhile to analyze their coordination chemistry towards the unusual Lewis acid trimeric (perfluoro-*ortho*-phenylene)mercury [(*o*-C₆F₄Hg)₃] (**3**).²⁴



Scheme 1. a) The planar Lewis acid **3** can simultaneously interact through all three Hg atoms with Lewis bases; b) Double-sandwich complexes built from **3** and the simple metallocenes [Cp₂Fe] and [Cp₂Ni].

The latter is a planar, electron deficient molecule containing three sterically available Hg atoms in close proximity. Compound **3** forms weak Lewis acid/base adducts with a large variety of O, N and S-donor Lewis bases as well as some anions (scheme 1 a).^{25,26} Additionally, it readily builds up alternating binary stacks with different electron rich aromatic hydrocarbons²⁷⁻³² and forms double-sandwich complexes with the metallocenes [Cp₂Ni] and [Cp₂Fe] (scheme 1 b).³³ Accordingly, we reported the reaction of **3** with the triple-decker complex [(CpMo)₂(μ,η⁶:η⁶-P₆)] bearing two Cp rings and a *cyclo*-P₆ middle-deck.³⁴ In this case, the obtained products show a one-dimensional polymeric structure which are based on weak P-Hg interactions and no Hg-Cp interactions are observed.

The presented results raise the question how the ferrocene analog *cyclo*-E₅ complexes **1** and **2** will interact with the planar Lewis acid **3**. Will they form Lewis acid/base adducts via the lone pairs of the group 15 elements or will they show a π interaction of the aromatic E₅ ligands comparable to pure ferrocene? To address this question we reacted the *cyclo*-E₅ complexes **1** and **2** with [(*o*-C₆F₄Hg)₃] (**3**) in CH₂Cl₂ and subsequently determined the solid state structure of the products. To gain further insight into the Hg–E interactions, the electrostatic potentials of the complexes **1-3** were obtained from DFT calculations. Additionally an atoms in molecules (AIM) analyses was performed at the experimentally determined geometries. To investigate the impact of sterical demand to these compounds, we prepared a series of *cyclo*-P₅ sandwich complexes [Cp^RFe(η⁵-P₅)] (Cp^R = C₅H_{5-*n*}tBu_{*n*}, *n* = 1-3, **6 a-c**) with increasing sizes of the Cp ligands and subsequently reacted them with compound **3**.[†] The resulting adducts were analysed by X-ray crystallography and a Hirshfeld surface analysis was performed to better compare the involved intermolecular contacts in the solid state.

Results and discussion

Synthesis of the compounds **4**, **5**, **7 a-c**

Since [(*o*-C₆F₄Hg)₃] (**3**) forms Lewis acid/base adducts with donor solvents like THF or MeCN, the syntheses were all conducted in CH₂Cl₂ to prevent any competition between the E_{*n*} ligand complexes and the solvent molecules. Nevertheless, in some other reactions we could isolate two solvates of [(*o*-C₆F₄Hg)₃] containing only CH₂Cl₂ (see supporting information). For the current study, the E_{*n*} ligand complexes were combined with a stoichiometric (1:1) amount of [(*o*-C₆F₄Hg)₃] and the mixture was dissolved in pure CH₂Cl₂. After filtration the solvent was evaporated to the limit of solubility. The supersaturated solution was stored at +4 °C or –30 °C which afforded crystals of the compounds **4**, **5** and **7 a-c** in a matter of several hours to some days.

Synthesis of the sandwich complexes [Cp^RFe(η⁵-P₅)] (Cp^R = C₅H_{5-*n*}tBu_{*n*}, *n* = 1-3, **6 a-c**)

For the present work all three complexes were prepared by a thermolysis of [Cp^RFe(CO)₂]₂ with P₄ in decalin. Chromatographic workup afforded the pure compounds as dark green solids.

General considerations

The solid state structures of the formed assemblies are based on weak interactions of the Hg atoms of [(*o*-C₆F₄Hg)₃] and the phosphorus or arsenic atoms of the sandwich complexes [Cp^RFe(η⁵-E₅)]. The van der Waals (vdW) radius of Hg in different compounds is discussed in the literature with reported values ranging from 1.7 Å up to 2.2 Å.³⁵⁻³⁸ In the following discussion the shortest value of 1.7 Å is taking as a reference. Therefore, Hg–E distances that are within the sum of the vdW radii³⁹ of 3.6 Å for E = P or 3.7 Å for E = As are highlighted by fragmented blue lines in the following figures 1, 2 and 6.

When the starting compounds **1** and **3** are dissolved in CH₂Cl₂, the solution shows the dark green color of the pure complex **1**. The crystals which were obtained by storing a concentrated solution at –30 °C are pleochromic showing a green to brown color. Compound **4** crystallizes in the triclinic space group *P*1̄. The solid state structure is depicted in figure 1.

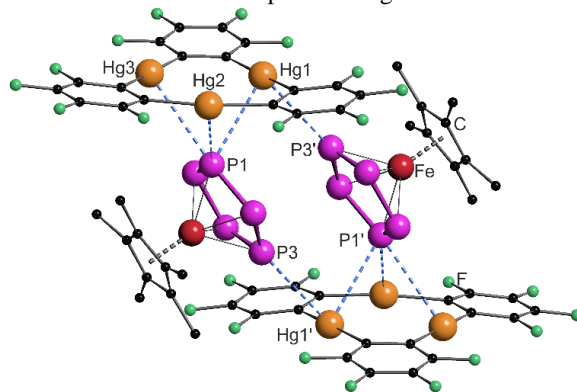


Fig 1 Solid state structure of **4**; selected bond lengths [Å] and angles [°]: Hg1-P1 3.2878(9), Hg2-P1 3.3592(9), Hg3-P3 3.5281(11), Hg1'-P3 3.5265(10), angle P₅-plane - Hg₃-plane 62.29(2).

In **4** the P₅ ring of **1** is approaching the center of the three Hg atoms of **3** with the phosphorus atom P1 and on the other side, the atom P3 is coordinating to the second Hg₃ moiety. The P-P bond lengths are very uniform with an average value of 2.111(4) Å, which is the same as in the starting compound **1** with 2.120(5) Å.²¹ The angle enclosed by the *cyclo*-P₅ plane and the Hg₃ plane constitutes 62.29(2)°. The observed assembly resembles the weak Lewis acid/base adducts that are formed from **3** with several Lewis bases and significantly differs from a cofacial arrangement that was found for the double-sandwich complexes formed by [Cp₂Fe] and **3**.³³ The closest Hg-P distance Hg1-P1 of 3.2878(9) Å is a bit longer than the closest Hg-P contact (3.195(3) Å) found in the polymeric chains of [(*o*-C₆F₄Hg)•{(CpMo)₂(μ,η⁶:η⁶-P₆)}]_{*n*} but the other found Hg-P distances can be compared well with this

one.³⁴ The shortest intermolecular P...P distance is 3.9443(13) Å and all others lie above 4 Å. In summary, the best description of the solid state structure of **4** is the enclosure of two *cyclo*-P₅ sandwich complexes by two planar molecules of **3** held together by weak Hg...P interactions.

In CD₂Cl₂ solution at room temperature **4** shows a singlet in both the ¹H NMR spectrum and the ³¹P{¹H} NMR spectrum. The signal is only shifted 0.04 ppm upfield in the case of the methyl protons and 2.5 ppm downfield in the case of the phosphorus atoms compared to the free complex **1**. When going to 193 K, these shifts increase to 0.13 ppm upfield for the ¹H and 7.6 ppm downfield for the ³¹P nuclei. In all experiments we could not resolve any coupling to the NMR active ¹⁹⁹Hg (*I* = 1/2, 16.84% natural abundance) or ²⁰¹Hg (*I* = 3/2, 13.22% natural abundance) nuclei. The ¹⁹F NMR spectrum shows two multiplets that correspond to the fluorine atoms of **3** in *ortho* and *para* position to the Hg atoms.⁴⁰ The mass spectrum (FD or ESI) of **4** shows no adduct in the gas phase. Only the starting materials **1** and **3** can be detected. Thus, the small differences of the chemical shifts and the absence of any coupling in the NMR spectra as well as the absence of any product peaks in the mass spectrum are in good agreement with the expected weak Hg...P interactions.

During the further investigation we also added the *cyclo*-As₅ complex **2** to the Lewis acid **3**. The brown solution of both compounds in CH₂Cl₂ could easily be distinguished from the olive green color of the pure sandwich complex **2**. The obtained crystals of compound **5** show a medium brown color. The solid state structure is shown in figure 2.

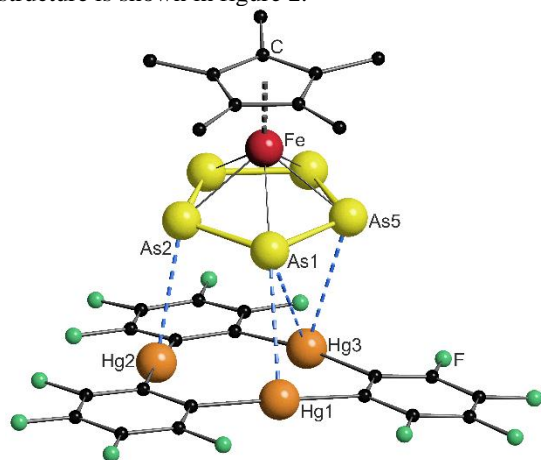


Fig 2. Solid state structure of **5**; selected bond lengths [Å] and angles [°]: Hg1-As1 3.4059(4), Hg2-As2 3.3014(4), Hg3-As1 3.6325(5), Hg3-As5 3.4201(5), angle As₅-plane - Hg₃-plane 10.68(2)

Compound **5** crystallizes in the triclinic space group *P1*. The As-As bond lengths are very uniform with an average value of 2.326(6) Å which is the same as found in the starting compound **2** (2.327(6) Å).²³ The assembly of the As₅ ring significantly differs from the P₅ ring in **4**. The angle enclosed by the As₅ plane and the Hg₃ plane of 10.68(2) ° shows an almost parallel arrangement. The center of the Hg₃ triangle is not situated directly below the center of the As₅ ring, but rather to

the arsenic atom As1. The resulting Hg-As distances show four contacts below the sum of the vdW radii with the closest one between Hg2 and As2 with 3.3014(4) Å. The assembly can best be described as a coordination of three As atoms to the Hg₃ platform. The observation of different assemblies for **1** and **2** with the weak Lewis acid **3** was surprising, since we observed a similar η⁵-coordination mode of the E₅ end-decks of **1** and **2** to the weak Lewis acids Tl⁺ and In⁺ before.²³ There is no second molecule of **3** stacked directly on top of the sandwich complex **2** to form a double-sandwich structure like it was observed for ferrocene. Nevertheless, there is a close contact (3.383(2) Å) of a carbon atom of the Cp* ring to a carbon atom of a fluorinated phenyl ring of the next molecule of **3** which may indicate possible stabilizing π-π-interaction of the electron rich Cp* ring to the electron deficient molecules of **3** or even F-H interaction to the methyl groups.

In order to better understand the difference in the nature of the Hg-E interactions in **4** and **5**, their constituent compounds **1**, **2**, and **3** were first subjected to optimization by DFT methods.^{††} The computed magnitudes of the respective HOMO-LUMO gaps between **1** and **3** and **2** and **3** of 3.70 and 3.36 eV suggest that efficient mixing of the HOMOs of **1** and **2** with the LUMO of **3** is not likely to be prevalent in **4** and **5**. Instead, we envisage that electrostatic and dispersion forces may play a large role in the stabilization of these adducts. To investigate the role played by electrostatic forces in **4** and **5**, we decided to inspect the electrostatic potential surfaces of the individual components shown in figure 3. For **1** and **2**, a distinct accumulation of negative character is observed at the center of the E₅ ring. This feature is reminiscent of that observed for simple aromatic units such as benzene or the cyclopentadienide ligands of metallocenes.⁴¹ A closer inspection of the surfaces shows a greater accumulation of negative character at the phosphorus atoms in **1**. This accumulation of negative character appears to be directly aligned with the phosphorus lone pairs that point outward from the center of the P₅ ring. Such areas of negative electrostatic potential concentrations are much less developed on the surface of the As₅ ring in **2**, a difference that we assign to the more electropositive character of arsenic and the more diffuse nature of its orbitals. Bearing in mind that the electrostatic potential surface at the center of the **3** is positive,^{26,42} formation of the adducts **4** and **5** is driven, at least in part, by electrostatic forces as shown by the complementarity of the surfaces that come into contact in the adducts.

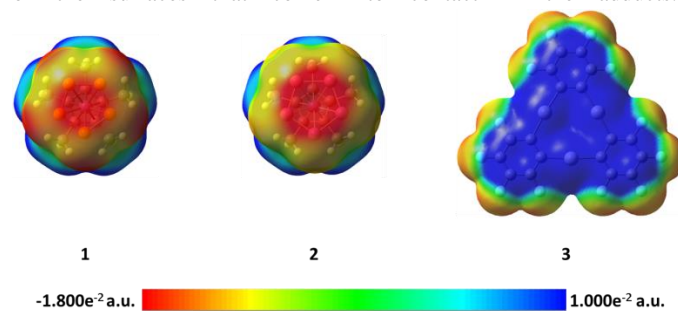


Fig 3. Electrostatic potential surfaces of compounds **1**, **2**, and **3**.

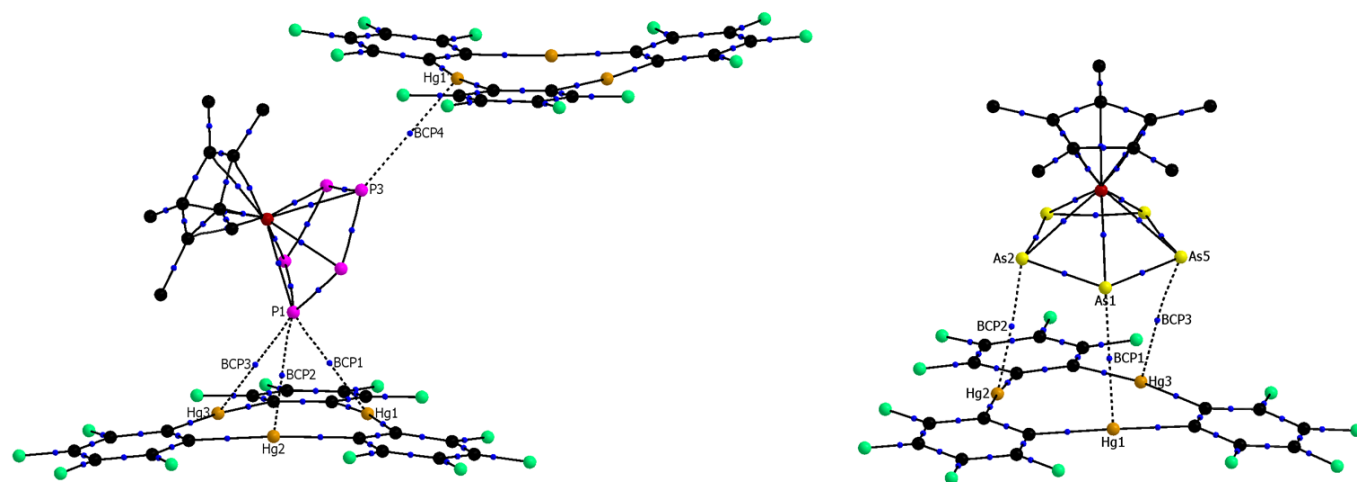


Fig. 4. Sections of the solid state structure of **4** (left) and **5** (right), including selected bond critical points located via AIM analysis. Bond critical points are shown in blue.

Table 1. Calculated features of the electron density distribution at selected BCPs in **4**.

BCP No. (A-B)	$d(\text{A-BCP})$ (Å)	$d(\text{B-BCP})$ (Å)	$\rho(r_{\text{BCP}})$ ($e \text{ \AA}^{-3}$)	$\nabla^2\rho(r_{\text{BCP}})$ ($e \text{ \AA}^{-5}$)	$H(r_{\text{BCP}})/\rho(r_{\text{BCP}})$ ($E_{\text{h}} e^{-1}$)	ϵ
1 (Hg1-P1)	1.657	1.630	0.105	0.876	0.012	0.048
2 (Hg2-P1)	1.664	1.696	0.101	0.835	0.020	0.046
3 (Hg3-P1)	1.754	1.776	0.072	0.620	0.055	0.046
4 (Hg1'-P3)	1.737	1.789	0.072	0.622	0.065	0.051

Table 2. Calculated features of the electron density distribution at selected BCPs in **5**.

BCP No. (A-B)	$d(\text{A-BCP})$ (Å)	$d(\text{B-BCP})$ (Å)	$\rho(r_{\text{BCP}})$ ($e \text{ \AA}^{-3}$)	$\nabla^2\rho(r_{\text{BCP}})$ ($e \text{ \AA}^{-5}$)	$H(r_{\text{BCP}})/\rho(r_{\text{BCP}})$ ($E_{\text{h}} e^{-1}$)	ϵ
1 (Hg1-As1)	1.698	1.707	0.091	0.757	0.044	0.031
2 (Hg2-As2)	1.654	1.648	0.109	0.885	0.018	0.052
3 (Hg3-As5)	1.695	1.731	0.096	0.762	0.027	0.344

The side-on coordination of the phosphorus complex **1** to the center of **3** in adduct **4** can be correlated to the concentration of negative charges on each of the phosphorus atoms. Similarly, the more co-planar arrangement of the As_5 ring and Hg_3 plane in **5** is proposed to result from the complementarity of the negative and positive electrostatic potential concentration at the centers of the As_5 and Hg_3 units, respectively.

In an effort to further investigate the nature of the Hg-E interactions in **4** and **5**, atoms in molecules (AIM)⁴³ analyses were carried out at the experimentally determined geometries. XYZ plots featuring selected bond critical points between the *cyclo-Es* units and **3** are shown in figure 4. Relevant features of the calculated electron density distributions for selected Hg-E bond critical points (BCP) found in **4** and **5** are shown in tables **1** and **2**, respectively. Tables of the electron density distribution features at all bond critical points found between units of **1** and **3** and **2** and **3** are provided in the supporting information. In **4**, four bond critical points were found between the *cyclo-P5* moiety of **1** and the two molecules of **3**, as shown in figure 4. P1, which is positioned above the center of a unit of **3**, shares a BCP with each of the proximal Hg atoms, with the electron densities at the critical points ranging from 0.072 to 0.105 $e \text{ \AA}^{-3}$.

A critical point with similar electron density (0.072 $e \text{ \AA}^{-3}$) was also found between P3 and Hg1' of the second unit of **3**. In **5**, AIM analysis found three BCPs between the *cyclo-As5* moiety of **2** and **3**. The three As atoms closest to **3** (As1, As2, and As5) each share a single critical point with a proximal Hg atom, with the electron densities at these critical points ranging from 0.091 to 0.109 $e \text{ \AA}^{-3}$.

The values of the electron density, $\rho(r)$, found at the Hg-E BCPs in both **4** and **5** are relatively small, being similar in magnitude to those found for weak hydrogen bonds.⁴⁴ The positive values of the Laplacian of the electron density at the Hg-E BCPs, $\nabla^2\rho(r_{\text{BCP}})$, are also suggestive of closed shell interactions. The relatively small magnitude of the $\rho(r)$ and $\nabla^2\rho(r_{\text{BCP}})$ values found at the bond critical points are not conclusive evidence of the weakness of the Hg-E interactions, as $\rho(r)$ values tend to become smaller with increasing diffuseness of the electrons involved.⁴⁵ However, the positive values of $H(r_{\text{BCP}})/\rho(r_{\text{BCP}})$, the total energy density at the BCP relative to $\rho(r)$,⁴³ found at the Hg-E BCPs suggest that any donor-acceptor^{46,47} contribution to the Hg-E bonding is weak.⁴⁸ Instead, we note that positive $H(r_{\text{BCP}})/\rho(r_{\text{BCP}})$ values are usually encountered in systems stabilized by electrostatic and/or van

der Waals interactions.⁴⁵ Hence, while donor-acceptor bonding cannot be entirely neglected in **4** and **5**, electrostatic forces as supported by the preceding potential map analysis must play a prevalent role in the formation of these adducts. Dispersion forces, which are inherently more difficult to visualize, may also play an important role.

The ellipticity values (ϵ), which provide information on the anisotropy of electron density perpendicular to the bond path, at the Hg-P BCPs in **4** are small and uniform, indicating no preferential plane of electron density accumulation. This is a characteristic of σ interactions, in agreement with the orientation of the phosphorus lone pairs toward the mercury atoms. In contrast to those found in **4**, the ellipticities at the Hg-As BCPs in **5** are not uniform. The ellipticity value of 0.344 found at the BCP between Hg3 and As5 is substantially larger than the values obtained for the two other Hg-As BCPs. Considering the relative uniformity of the $\rho(r)$ values found for all three Hg-As BCPs, the large ellipticity value found for the Hg3-As5 BCP suggests the involvement of an As-As π -bond in the interaction with Hg3.

Whether the different assembly of the *cyclo*-P₅ and the *cyclo*-As₅ complexes towards the planar Lewis acid **3** might be caused by packing effects due to the longer As-As bonds (≈ 2.33 Å) compared to the P-P bonds (≈ 2.12 Å) is hard to answer. Considering all the presented experimental data we can assume the Hg...P interactions found in **4** to be weak. Both E₅ complexes **1** and **2** exhibit two degenerate orbitals as their HOMO which are localized on the E₅ rings.²⁰ Consequently, we rationalized that it might be possible to direct the P₅ complex to also show an almost cofacial arrangement to the molecular plane of the Lewis acid **3**. Therefore, we followed a synthetic approach by increasing the steric bulk of the Cp^R ligand on the *cyclo*-P₅ sandwich complex to induce a change of its orientation towards the Hg₃ plane of **3** in the solid state. For this reason we decided to compare complexes with mono-, di- and trisubstituted *tert*-butyl-cyclopentadienyl ligands [Cp^RFe(η^5 -P₅)] (**6 a**), [Cp^RFe(η^5 -P₅)] (**6 b**), [Cp^RFe(η^5 -P₅)] (**6 c**). The compounds are obtained by reacting the suitable Cp^R substituted dimeric iron-dicarbonyl complexes [Cp^RFe(CO)₂]₂ with white phosphorus at elevated temperature.

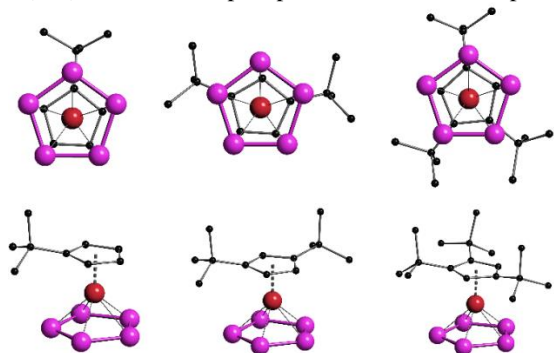


Fig 5. Solid state structures of the complexes [Cp^RFe(η^5 -P₅)] **6 a** (left), [Cp^RFe(η^5 -P₅)] **6 b** (middle), [Cp^RFe(η^5 -P₅)] **6 c** (right); (top) viewing direction perpendicular to the P₅ plane revealing a nearly eclipsed arrangement of the

Cp rings to the P₅ rings for all three complexes. (bottom) side view of the complexes **6 a-c**.

The determined solid state structures of **6 a-c** are shown in figure 5. All three analyzed complexes **6a-c** show the expected sandwich structure with two parallel five-membered rings. Table 1 summarizes some geometric data for a better comparison. The distances between the Fe atom and the center of both rings are increasing very little when the size of the Cp ligand is increasing. When looking at the top row in figure 5 it can be seen that the P₅ rings are almost in eclipsed position with the Cp rings in all cases. This could be explained by steric effects when looking closer at the bottom row, since two methyl groups of each *tert*-butyl group are pointing between two P atoms of the P₅ rings. The volume of the complexes was determined by dividing the unit cell volume by the number of molecules within the cell. Here it can be seen, that each additional *tert*-butyl group adds about 100 Å³ to the size of the complexes.

Table 3. Selected lengths [Å]: $d(P_5-Fe)$ and $d(Cp-Fe)$ describe the distances of Fe to the center of the five-membered rings.

	$d(P_5-Fe)$	$d(Cp-Fe)$	volume/Å ³
6 a	1.5396(2)	1.7026(2)	338.6
6 b	1.5514(13)	1.7122(13)	436.5
6 c	1.5615(2)	1.7174(2)	530.2

With these *cyclo*-P₅ complexes **6a-c** in hand, we prepared and fully characterized the compounds **7a-c** formed in the reaction of the *cyclo*-P₅ complex with [(*o*-C₆F₄Hg)₃] in a 1:1 stoichiometry. The solid state structures of **7a-c** are shown in figure 6. The obtained compounds each exhibit a similar assembly like it was found in **4** with two *cyclo*-P₅ complexes enclosed by two molecules of **3** held together by weak Hg...P interactions.

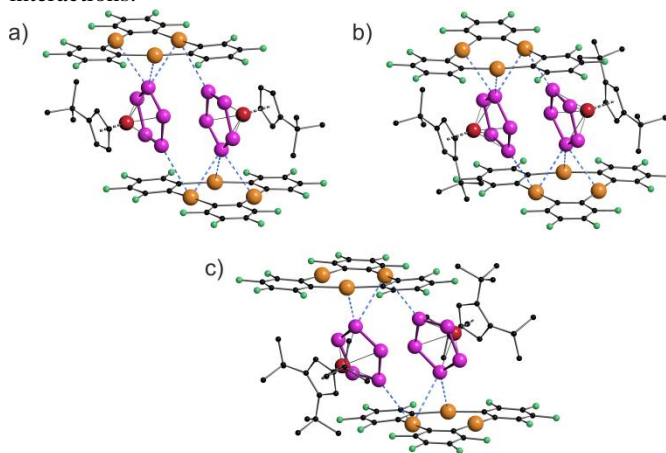


Fig 6. Solid state structures of [(Cp^RFe(η^5 -P₅))₂•{(*o*-C₆F₄Hg)₃}] (**7a**) (a), [(Cp^RFe(η^5 -P₅))₂•{(*o*-C₆F₄Hg)₃}] (**7b**) (b), [(Cp^RFe(η^5 -P₅))₂•{(*o*-C₆F₄Hg)₃}] (**7c**) (c);

There are small differences in the assemblies caused by the steric demand of the Cp ligands, but the general arrangement of the *cyclo*-P₅ ring towards the molecular plane of **3** did not change dramatically, although the central phosphorus atom in

7c (figure 6 c) shows only two contacts below the sum of the vdW radii to the Hg atoms of **3**.

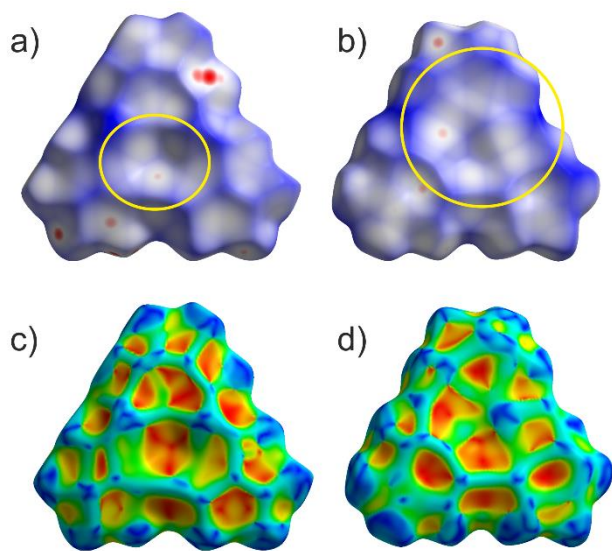


Fig 7. Representation of the Hirshfeld surfaces (HS) of the planar Lewis acid **3** in compounds **4** (a + c) and **5** (b + d). The first row shows d_{norm} values mapped onto the HS while the second row shows the shape index. Highlighted in yellow are the contact areas of the planar molecule **3** with the *cyclo-E₅* ligands of [Cp*Fe(η^5 -P)₅] in a) and [Cp*Fe(η^5 -As)₅] in b), respectively.

In order to better visualize the different interaction of the *cyclo-P₅* and the *cyclo-As₅* ligand towards the planar Lewis acid **3** we performed a Hirshfeld surface analysis^{49,52} of all described compounds.⁵³ Figure 7 shows a representation of the Hirshfeld surfaces (HS) of the planar Lewis acid **3** which is facing the *cyclo-E₅* ligands **1** or **2** derived from the solid state structures of **4** (a + c) and **5** (b + d), respectively. While the first row shows d_{norm} values which are used to identify close intermolecular contacts mapped onto the HS, the second row displays the corresponding shape index. The yellow ellipses highlight the contact regions to the pnictogen atoms of the *cyclo-E₅* ligands. Figure 7 a and c exhibit a pronounced indentation of the HS in the center of the molecule for **4**. Figure 7 a additionally shows three close contacts as white to red dots in this region on the HS which arise from interaction of the three Hg atoms of **3** with one P atom of the P₅ ring.⁵⁴ In figure 7 b we can identify a contact area, highlighted in yellow, which shows five small indentations for **5** instead. These can be seen even better in the representation of the respective shape index in figure 7 d, which resembles a rather face to face arrangement of the As₅ plane to the Hg₃ plane.

A detailed HS analysis including decomposed fingerprint plots of all described compounds enabled us to further analyze and compare important intermolecular distances. Figure 8 shows the fingerprint plots of the planar Lewis acid **3** in **4** and **5** with highlighted regions of contact atom pairs.⁵³

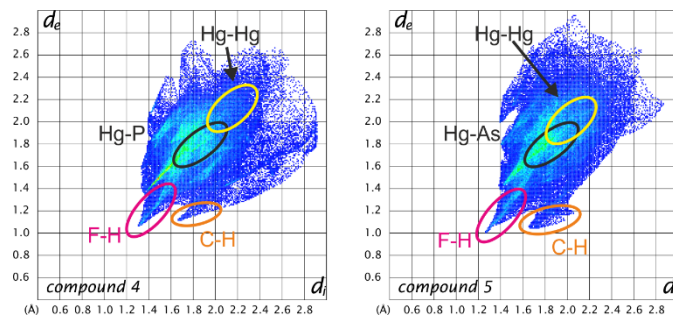


Fig 8. Fingerprint plots of the Hirshfeld surfaces of the planar Lewis acid **3** in the compounds **4** (left) and **5** (right); Regions of the shortest intermolecular distances depending on particular atom pairs are highlighted.

The fingerprint plots of the Lewis acid **3** show some similar features for all compounds. While F-H and C-H distances naturally represent the shortest intermolecular contacts, the Hg-Hg contacts are already at the edge of Hg-Hg interactions and only contribute less than 2% to the Hirshfeld surface. In **7c** there are no Hg-Hg contacts at all. However, the Hg-P and Hg-As distances represent short intermolecular contacts for their respective atom types below the sum of the vdW radii (see general considerations). The Hg-P contact area generally contributes about 4-5% to the Hirshfeld surface in all *cyclo-P₅* compounds (**4**, **7a-c**) and does not change upon Cp ligand exchange of the P₅ complexes. In contrast, the F-H and F-F contacts for example are significantly influenced by the respective *cyclo-P₅* complex (rising H content of the Cp ligand results in rising F-H contact area).⁵³ Therefore, in accordance with the single-crystal X-ray structure analyses, it can be assumed, that the observed arrangement in the solid state of two *cyclo-P₅* sandwich complexes enclosed by two planar Lewis acidic molecules **3** is relatively stable and it can resist a considerable increase in size of the adjacent ligands on the *cyclo-P₅* sandwich complexes.

Conclusion

A systematic comparison of the coordination behavior of the *cyclo-E₅* complexes [Cp*Fe(η^5 -P₅)] (**1**) and [Cp*Fe(η^5 -As₅)] (**2**) towards the planar trinuclear Lewis acid [(*o*-C₆F₄Hg)₃] (**3**) is presented. While one phosphorus atom of the P₅ ring of **1** interacts simultaneously with all three Hg atoms of **3** resembling a weak Lewis acid/base adduct, the analogous *cyclo-As₅* complex **2** is interacting with the Hg atoms of **3** via only three As atoms instead showing an almost cofacial arrangement of the As₅ plane to the Hg₃ plane of **3** in the solid state. The assemblies are supported by weak Hg-E interactions which are in agreement with the small shifts in the NMR spectra as well as the absence of any adduct signals in the mass spectra of **4** and **5**.

Large energy gaps between the HOMOs of **1** and **2** and the LUMO of **3**, along with the complementarity of their respective electrostatic potential surfaces, suggests that electrostatic forces play a prominent role in the stabilization and coordination behavior of **4** and **5**. AIM analyses of **4** and **5** corroborate the

observed weakness of the Hg-E interactions, and suggest the involvement of an As-As π bond in the Hg-*cyclo*-As interactions in **5**.

Subsequently, the *cyclo*-P₅ sandwich complexes **6 a-c** as well as their adducts with the Lewis acid **3 (7 a-c)** were prepared and fully characterized. By determining the solid state structure and performing a detailed Hirshfeld surface analysis for all compounds we could demonstrate that the general arrangement which was found for **4** is relatively stable and can resist a considerable increase of steric demand of the *cyclo*-P₅ complexes. A comparison of the HS of **4** and **5** shows quite different contact areas as expected.

In conclusion the presented results show that although the characterized compounds are only supported by weak interactions instead of strong covalent dative bonds the preference of the σ -interaction of the *cyclo*-P₅ complex **1** and π -interaction of the *cyclo*-As₅ complex **2** is observed.

Acknowledgements

This work was financially supported by the Deutsche Forschungsgemeinschaft (Sche 384/26-2), the National Science Foundation (CHE-1300371) and the Welch Foundation (A-1423). Christian Marquardt is gratefully acknowledged for recording the crystal data for [**3**•(CH₂Cl₂)] (**9**) (see supporting information). Bianca Attenberger is acknowledged for recording the analytical data for [Cp*FeP₅] **6 a**.

Notes and references

^a Institut für Anorganische Chemie, Universität Regensburg, 93040 Regensburg, Germany, manfred.scheer@chemie.uni-regensburg.de Fax: (+49) 941-943-4439

^b Department of Chemistry, Texas A&M University, College Station, Texas 77843-3255, USA

† The complexes for $n = 2, 3$ were reported before.^{55,56} During this work the first solid state structure for a complex with $n = 2$ and a new polymorph for $n = 3$ could be analyzed by X-ray diffraction analysis.

†† Calculations were performed using the Gaussian program with the B3LYP functional and mixed basis sets: Hg, cc-pVTZ-PP; P/Fe/As, 6-311++G**; F, 6-31G(d*); C/H, 6-31G).

Details of all X-ray structure analysis can be found in the supplementary information. CCDC-1012615-1012624.

Electronic Supplementary Information (ESI) available: details of the syntheses, X-ray diffraction analyses of all presented and related products and details of the DFT calculations; See DOI: 10.1039/b000000x/

- B. M. Cossairt, N. A. Piro and C. C. Cummins, *Chem. Rev.*, 2010, **110**, 4164-4177.
- M. Caporali, L. Gonsalvi, A. Rossin and M. Peruzzini, *Chem. Rev.*, 2010, **110**, 4178-4235.
- B. P. Johnson, G. Balázs and M. Scheer, *Coord. Chem. Rev.*, 2006, **250**, 1178-1195.
- O. J. Scherer, *Angew. Chem. Int. Ed.*, 1990, **29**, 1104-1122.
- O. J. Scherer, *Acc. Chem. Res.*, 1999, **32**, 751-762.
- D. Y. Zubarev and A. I. Boldyrev, in *Encyclopedia of Inorganic and Bioinorganic Chemistry*, John Wiley & Sons, Ltd, 2011.
- N. H. Martin and J. D. Robinson, *J. Mol. Graphics Modell.*, 2012, **38**, 26-30.
- Z. Li, C. Zhao and L. Chen, *J. Mol. Struct.*, 2007, **810**, 1-6.
- F. De Proft, P. W. Fowler, R. W. A. Havenith, P. v. R. Schleyer, G. Van Lier and P. Geerlings, *Chem. Eur. J.*, 2004, **10**, 940-950.
- E. J. P. Malar, *J. Org. Chem.*, 1992, **57**, 3694-3698.
- O. J. Scherer and T. Brück, *Angew. Chem. Int. Ed.*, 1987, **26**, 59-59.
- O. J. Scherer, C. Blath and G. Wolmershäuser, *J. Organomet. Chem.*, 1990, **387**, C21-C24.
- J. Bai, A. V. Virovets and M. Scheer, *Angew. Chem. Int. Ed.*, 2002, **41**, 1737-1740.
- F. Dielmann, A. Schindler, S. Scheuermayer, J. Bai, R. Merkle, M. Zabel, A. V. Virovets, E. V. Peresykina, G. Brunklaus, H. Eckert and M. Scheer, *Chem. Eur. J.*, 2012, **18**, 1168-1179.
- J. Bai, A. V. Virovets and M. Scheer, *Science*, 2003, **300**, 781-783.
- M. Scheer, A. Schindler, C. Gröger, A. V. Virovets and E. V. Peresykina, *Angew. Chem. Int. Ed.*, 2009, **48**, 5046-5049.
- M. Scheer, A. Schindler, J. Bai, B. P. Johnson, R. Merkle, R. Winter, A. V. Virovets, E. V. Peresykina, V. A. Blatov, M. Sierka and H. Eckert, *Chem. Eur. J.*, 2010, **16**, 2092-2107.
- S. Welsch, C. Gröger, M. Sierka and M. Scheer, *Angew. Chem. Int. Ed.*, 2011, **50**, 1435-1438.
- A. Schindler, C. Heindl, G. Balázs, C. Gröger, A. V. Virovets, E. V. Peresykina and M. Scheer, *Chem. Eur. J.*, 2012, **18**, 829-835.
- H. Krauss, G. Balázs, M. Bodensteiner and M. Scheer, *Chem. Sci.*, 2010, **1**, 337-342.
- M. Scheer, L. J. Gregoriades, A. V. Virovets, W. Kunz, R. Neueder and I. Krossing, *Angew. Chem. Int. Ed.*, 2006, **45**, 5689-5693.
- S. Welsch, L. J. Gregoriades, M. Sierka, M. Zabel, A. V. Virovets and M. Scheer, *Angew. Chem. Int. Ed.*, 2007, **46**, 9323-9326.
- M. Fleischmann, S. Welsch, H. Krauss, M. Schmidt, M. Bodensteiner, E. V. Peresykina, M. Sierka, C. Gröger and M. Scheer, *Chem. Eur. J.*, 2014, **20**, 3759-3768.
- P. Sartori and A. Golloch, *Chem. Ber.*, 1968, **101**, 2004-2009.
- M. R. Haneline, R. E. Taylor and F. P. Gabbai, *Chem. Eur. J.*, 2003, **9**, 5188-5193.
- T. J. Taylor, C. N. Burress and F. P. Gabbai, *Organometallics*, 2007, **26**, 5252-5263.
- T. J. Taylor, C. N. Burress, L. Pandey and F. P. Gabbai, *Dalton Trans.*, 2006, 4654-4656.
- C. N. Burress, M. I. Bodine, O. Elbjairami, J. H. Reibenspies, M. A. Omary and F. P. Gabbai, *Inorg. Chem.*, 2007, **46**, 1388-1395.
- A. S. Filatov, E. A. Jackson, L. T. Scott and M. A. Petrukhina, *Angew. Chem. Int. Ed.*, 2009, **48**, 8473-8476.
- M. Tsunoda and F. P. Gabbai, *J. Am. Chem. Soc.*, 2000, **122**, 8335-8336.
- M. R. Haneline, M. Tsunoda and F. P. Gabbai, *J. Am. Chem. Soc.*, 2002, **124**, 3737-3742.
- M. R. Haneline, J. B. King and F. P. Gabbai, *Dalton Trans.*, 2003, 2686-2690.
- M. R. Haneline and F. P. Gabbai, *Angew. Chem., Int. Ed.*, 2004, **43**, 5471-5474.
- M. Fleischmann, C. Heindl, M. Seidl, G. Balázs, A. V. Virovets, E. V. Peresykina, M. Tsunoda, F. P. Gabbai and M. Scheer, *Angew. Chem. Int. Ed.*, 2012, **51**, 9918-9921.
- A. J. Canty and G. B. Deacon, *Inorg. Chim. Acta*, 1980, **45**, L225-L227.
- S. S. Batsanov, *J. Chem. Soc., Dalton Trans.*, 1998, 1541-1546.
- P. Pyykko and M. Straka, *PCCP*, 2000, **2**, 2489-2493.
- K. R. Flower, V. J. Howard, S. Naguthney, R. G. Pritchard, J. E. Warren and A. T. McGown, *Inorg. Chem.*, 2002, **41**, 1907-1912.
- A. F. Holleman, E. Wiberg and N. Wiberg, *Lehrbuch der Anorganischen Chemie*, Walter de Gruyter, Berlin, 2007.
- R. E. Taylor and F. P. Gabbai, *J. Mol. Struct.*, 2007, **839**, 28-32.
- J. Rodríguez-Otero, E. M. Cabaleiro-Lago, Á. Peña-Gallego and M. Merced Montero-Campillo, *Tetrahedron*, 2009, **65**, 2368-2371.
- A. Burini, J. P. Fackler, R. Galassi, T. A. Grant, M. A. Omary, M. A. Rawashdeh-Omary, B. R. Pietroni and R. J. Staples, *J. Am. Chem. Soc.*, 2000, **122**, 11264-11265.
- R. W. F. Bader, *Atoms in Molecules. A Quantum Theory*, Cambridge University Press, Oxford, UK, 1991.
- R. Parthasarathi, V. Subramanian and N. Sathyamurthy, *J. Phys. Chem. A*, 2006, **110**, 3349-3351.

- 45 P. Macchi and A. Sironi, *Coord. Chem. Rev.*, 2003, **238–239**, 383-412.
- 46 G. Frenking, *Angew. Chem. Int. Ed.*, 2014, **53**, 6040-6046.
- 47 D. Himmel, I. Krossing and A. Schnepf, *Angew. Chem. Int. Ed.*, 2014, **53**, 370-374.
- 48 D. Cremer and E. Kraka, *Angew. Chem. Int. Ed.*, 1984, **23**, 627-628.
- 49 J. J. McKinnon, D. Jayatilaka and M. A. Spackman, *Chem. Commun.*, 2007, 3814-3816.
- 50 J. J. McKinnon, A. S. Mitchell and M. A. Spackman, *Chem. Eur. J.*, 1998, **4**, 2136-2141.
- 51 M. A. Spackman and D. Jayatilaka, *Crystengcomm*, 2009, **11**, 19-32.
- 52 M. A. Spackman, *Phys. Scr.*, 2013, **87**, 48103.
- 53 A detailed discussion of the Hirshfeld surface analyses for the compounds **4**, **5** and **7a-c** can be found in the supporting information including representations of discussed surfaces and selected decomposed fingerprint plots.
- 54 Unfortunately, the close contacts are not very pronounced as red contact areas since the crystal explorer software uses shorter vdW radii as a reference. A detailed description of the matter can be found in the supporting information.
- 55 M. Scheer, G. Friedrich and K. Schuster, *Angew. Chem. Int. Ed.*, 1993, **32**, 593-594.
- 56 O. J. Scherer, T. Hilt and G. Wolmershäuser, *Organometallics*, 1998, **17**, 4110-4112.